TRAVEL TIME CURVES AT SMALL DISTANCES, AND WAVE VELOCITIES IN SOUTHERN CALIFORNIA.

By

B. Gutenberg, Pasadena (Calif.).

(With 11 figures.)

Zusammenfassung: Das Netz von Erdbebenwarten in Kalifornien (table I) ermöglicht nunmehr eine genauere Untersuchung der Erdbeben in Südkalifornien. 21 Stöße (table II) erwiesen sich als geeignet für genauere Untersuchungen. Für jeden wurde zunächst das Epizentrum unter Benutzung von Stationspaaren mit angenähert gleichen Eintrittszeiten berechnet, unter Zugrundelegung einer scheinbaren Wellengeschwindigkeit von 5.6 km/sec für $\overline{P}$ nach den Ergebnissen von Steinbruchsprengungen daselbst (16). Unter Benutzung der so gefundenen Herddistanzen wurde die Laufzeitkurve für alle $\overline{P}$-Einsätze konstruiert, und mit dieser Laufzeitkurve wurden erneut die Koordinaten der Herde sowie die Herdzeiten berechnet (table II, III und Figur 1). Die Wiederholung des Verfahrens ergab keine wesentlichen Änderungen. Im ganzen standen 138 Aufzeichnungen (table IV), meist mit je zwei, zum Teil (Pasadena) auch wesentlich mehr Komponenten, zur Verfügung, mit zusammen 303 Kurven. Die Untersuchung der $\overline{P}$-Wellen ergab keinen wesentlichen Einfluß der Herdlage (table V). Dagegen zeigte sich, daß die Laufzeitkurve von $\overline{P}$ nur zwischen 200 und 450 km Herddistanz durch eine Gerade, entsprechend einer scheinbaren Geschwindigkeit von 5.55 km/sec, dargestellt werden konnte. Für kleinere Distanzen ist die Abweichung der Beobachtungen von dieser Geraden positiv (table VI), für größere stärker negativ. Die mittlere Kurve entspricht etwa dem Mittel der Laufzeitkurven von A. Mohorovičić für die Herdtiefen 0 und 25 km (table VII). P_n ließ sich bis 554 km Herddistanz verfolgen. Seine scheinbare Geschwindigkeit ist 7.94 km/sec mit ganz geringen Fehlern (table VIII). (In den Tabellen sind die Diagramme immer mit zwei Buchstaben bezeichnet, von denen sich der erste auf die Station, der zweite auf das Beben bezieht. Die Symbole sind die gleichen wie in table II bzw. III.) Die Laufzeitdifferenz $\overline{P}$—P_n ist in Kalifornien mehrere Sekunden größer, als bisher an anderen Stellen gefunden wurde (table IX). Kurz hinter P_n folgt die zuerst von V. Conrad festgestellte Welle P_x (table X), deren Amplituden merklich größer sind als die von P_n, und die in größeren Distanzen oft als erste Welle sichtbar ist. Sie folgt etwas schneller auf P_n, als V. Conrad beim Schwadorfer Beben fand (table XI). Zwischen P_n und $\overline{P}$ treten in nicht zu großen Distanzen zwei Wellen auf, die mit P_m und P_y bezeichnet wurden. P_m entspricht etwa der Welle P^* in europäischen Seismogrammen (table XII), es scheint aber nicht ausgeschlossen zu sein, daß auch in Europa verschiedentlich eine Welle beobachtet wurde, die P_y entspricht (Figur 4). Die scheinbaren Geschwindigkeiten dieser beiden Wellen, die oft sehr klar hervortreten (Figur 11), sind 6.83 bzw. 6.05 km/sec, ent-

sprechen also etwa den von BROCKAMP und WÖLCKEN (2) für Norddeutschland in den beiden obersten Schichten gefundenen Werten. Es ist daher denkbar, daß der Schichtenaufbau in Kalifornien qualitativ ähnlich ist wie in Europa, daß aber in Norddeutschland die oberste Schicht fehlt, während die P_y entsprechende Schicht in Süddeutschland und im Alpengebiet bisher noch nicht durch auffällige Wellen erkennbar war.

Außer diesen Wellen treten im Gebiete der Longitudinalwellen noch drei Wellen auf, die mit a, b und c bezeichnet wurden (table XIII); sie sind nur in größeren Distanzen erkennbar und zum Teil sogar sehr auffällig. Dies gilt besonders für a, dessen Laufzeit innerhalb der Beobachtungsgenauigkeit mit derjenigen einer von STONELEY (15) gefundenen Welle zusammenfällt. Die Laufzeitkurve dieser Welle kann jedoch nicht unter 200 km Distanz zurückverfolgt werden, und die Welle selbst kann keine Longitudinalwelle durch eine tiefere Schicht sein. Ein Versuch, die Entstehung dieser drei Wellen sowie zahlreicher anderer Wellen (table XVII) zu deuten, wurde angesichts der außerordentlich großen Zahl von möglichen reflektierten und gebrochenen sowie von Schichtgrenzen geführten Wellen nicht gemacht. Sobald die im Gang befindliche Ausrüstung aller Stationen des Netzes in Südkalifornien mit empfindlichen kurzperiodischen Vertikalseismometern durchgeführt ist, und Rechnungen über die Energieaufspaltung an Unstetigkeitsflächen weiter gediehen sind, verspricht die Behandlung dieser Probleme mehr Erfolg.

Bei der Untersuchung der Laufzeitkurve des vermutlichen $\overline{S}$ ergab sich keine analoge Krümmung wie bei $\overline{P}$. Es liegt daher die Möglichkeit vor, daß $\overline{S}$ völlig durch die Oberflächenscheerungswelle Q überdeckt wird (table XIV). Die den verschiedenen P-Wellen entsprechenden Wellen S_n, S_x, S_m und S_y sowie vereinzelt auch vermutlich die RAYLEIGH-Welle R treten oft deutlich hervor (table XVI). Die Kurve für S^* in Europa entspricht etwa der Kurve für S_y, das oft besonders kräftig ist, während das ebenfalls sehr kräftige S_m in Kalifornien eine ähnliche Laufzeitkurve hat, wie sie V. CONRAD für $\overline{S}$ des Schwadorfer Bebens gefunden hat.

Die Herdtiefe war makroseismisch in einigen Fällen nach einer von GASSMANN (6) angegebenen Formel der Größenordnung nach bestimmbar. Der Mittelwert von 12 km (table XVIIIa) stimmte gut zu den aus den Eintrittszeiten von $\overline{P}$ an Nahstationen berechneten Werten, die sich um eine Herdtiefe von 14 km gruppieren. Aus dem mittleren Kurvenverlauf von $\overline{P}$ (table VI) ergibt sich 10 km als wahrscheinlichster Wert. Unter Annahme einer Herdtiefe von 12 km ergibt sich schließlich 14 km als Dicke der obersten (Granit?-)Schicht. Ganz ähnlich wie in Europa würden also auch in Kalifornien die Herde nahe der unteren Grenze der Granitschicht liegen. Die aus den P- und S-Wellen berechneten Schichtdicken (Tabelle am Schlusse) stimmen gut miteinander überein.

I. The seismological stations.

The system of seismological stations in California now makes it possible to study local shocks with considerable accuracy in many cases. Records of the following stations were available for this purpose:

Pasadena, Seismological Laboratory, maintained and operated by the Carnegie Institution of Washington and the California Institute of Technology as a co-operative undertaking, and its six auxiliary stations at Mt. Wilson, Riverside, Santa Barbara, La Jolla, Tinemaha and Haiwee.

The stations at Berkeley and Lick Observatory (Mt. Hamilton) operated by the University of California.

The station at Tucson, Arizona, operated by the U. S. Coast and Geodetic Survey. All stations mentioned are equipped with Wood-Anderson torsion seismometers. The general direction of the instruments is N-S and E-W, but significant deviations from these directions occur in the case of torsion seismometers with short free periods; therefore in general it is not possible to use azimuths given by the seismograms. The free periods of these instruments were near 0.8 sec., at all stations except Tucson, the magnification for short waves near 3000 and the damping ratio nearly critical. At Tucson long period instruments of the same type are installed, with free periods near 10 seconds, and a magnification of 400—500 for short waves. At Pasadena similar instruments are used besides the short period type, and on many occasions

Table I. List of stations.

Station	Longitude N.	Latitude W.	Height m.	Foundation	Abbreviation
	° ′	° ′			
Pasadena . .	34 08.9	118 10.3	295	Weathered granite	P
Mt. Wilson . .	34 13.5	118 03.4	1742	Weathered granite	M
Riverside . .	33 59.6	117 22.4	250	Weathered granite	R
Santa Barbara	34 26.6	119 42.8	100	Alluvium	S
La Jolla . . .	32 51.8	117 15.2	8	Consolidated detrital material	J
Tinemaha . .	37 05.7	118 15.5	1180	Basalt	T
Haiwee . . .	36 08.2	117 58.6	1100	Loosely cemented tuff	H
Berkeley . .	37 52	122 16	85	Sandstone	B
Lick Obs. . .	37 20	121 39	1282	Feldspathic sandstone	L
Tucson . . .	32 15	110 50	770	Sand and gravel	U

vertical seismographs and wave seismographs both of the Benioff type were in service*).

*) These instruments were described at the Meeting of the Seismol. Soc. of America, held in Pasadena in June, 1931. The description will be published in the Bull. of the Seismol. Soc. of America.

In table I data on the stations are given. The location of most of them can be seen in figure 1. The time at the stations of the group in southern California is in general comparable within a small fraction of a second, the time marks being recorded at all stations on a separate sheet together with dots and dashes of one broadcasting station. Therefore the travel times between these stations are comparable without reference to absolute time. At Pasadena absolute time signals are generally registered three times a day; at Mt. Wilson (Riefler clock), Berkeley, and Lick Observatory once a day; at Tucson the time correction is kept near zero by changing the clock every day. The absolute time at all other stations is given by means of the radio system described above and the absolute times of Pasadena or Mt. Wilson, connected with this system.

II. The shocks.

The stations at Tinemaha and Haiwee were established in September, 1929. Therefore the investigations concern shocks which have occurred since that date. Only those shocks were used whose epicenter seemed to be certain within a very few km. Table II shows data on the shocks used for the following investigations.

The epicenter was found by the method which the author has used in some previous cases (7, 8). In general at least two pairs of stations can be found which have nearly the same time of arrival of $\bar{P}$-waves. The velocity of these waves had been found in southern Californis by Wood and Richter (16) to be near 5.6 km./sec. Therefore, if the $\bar{P}$-waves arrive at one station x seconds later than at another, the second station will be 5.6 x km. nearer to the epicenter than the first. The epicenter itself is known to a first approximation either by macroseismic data or by the time of arrival of the waves at different stations. We can therefore mark a point which is 5.6 x km. nearer to the epicenter than the first station, and the epicenter must be situated on the line which everywhere has the same distance from this point and the second station. A second pair of stations gives a second line, and their intersection a second approximation of the epicenter. If necessary, the method can now be repeated, using this better approximation to the epicenter. If one does not like this approximate method, he may construct hyperbolas, but the method described is more convenient and procures quicker results. Additional lines of this kind can now be obtained by using other pairs of stations.

Table II.

List of shocks.

Shock	Date	Longitude	Latitude	Time of origin (Greenw.)	Felt (r = mean radius of the shaken area, I = max. intensity)
		° ′	° ′	h m s	
A	Aug. 17, 1930 .	35 13	116 51	22 07 00.3	No reports (Mohave Dessert)
B	Sept. 26, 1929 .	34 50	116 31	20 00 22.7	r of the order 200 km.
C	May 29, 1930. .	35 30	117 14	7 12 16.0	No reports (Mohave Desert)
D	April 20, 1930 .	34 39	117 04	8 52 21.7	do.
E	Febr. 24, 1930 .	34 57	117 02	19 55 58.1	do.
F	Jan. 8, 1931. .	34 56	117 03	13 52 59.5	A few reports (Mohave Desert)
G	Jan. 16, 1930. .	34 11	116 55	0 24 33.9	r near 250 km., $I = 7°$. East of San Bernardino
H	Jan. 16, 1930. .	34 11	116 55	0 34 03.6	
J	April 23, 1931 .	35 25	117 36	23 34 07.3	North of Barstow (Mohave Desert)
K	April 27, 1931 .	34 21	116 17	23 07 58.6	Mohave Desert (29 Palms)
a	Oct. 31, 1929. .	33 38	118 12	19 39 23.6	Around Epic. $r = 20$ km.; $I = 4°$
b	Sept. 13, 1929 .	33 38	118 12	13 23 38.2	do. $r = 40$ „ $I = 5°$
c	Nov. 9, 1929 . .	35 46	120 28	2 30 42.1	do. $r = 60$ „ $I = 4°$
d	Aug. 31, 1930 .	33 56	118 37	0 40 36.0	Around Sta. Monica, $r = 150$ km., $I = 7°$
e	May 12, 1930. .	33 12	116 43	17 25 48.5	East La Jolla, $r = 40$ km, $I = 4°$
f	Jan. 17, 1931 . .	37 35	118 03	8 07 20.6	Nothing known (mountains)
g	Aug. 18, 1930 .	34 26	120 11	13 08 55.4	West of Santa Barbara, $r = 70$ km, $I = 5°$
h	Feb. 23, 1931. .	35 46	120 40	10 00 39.4	Around Epic. $r = 50$ km., $I = 4°$
i	April 24, 1931 .	33 46	118 29	18 27 54.8	do. Redondo, $r = 50$ „ $I = 6°$
k	April 21, 1931 .	35 19	118 55	19 26 41.5	South of Bakersfield
l	April 29, 1931 .	34 15	118 39	12 41 36.8	A few reports near epicenter

In the following investigations only shocks were used whose epicenters could be found by this method. Therefore table II does not

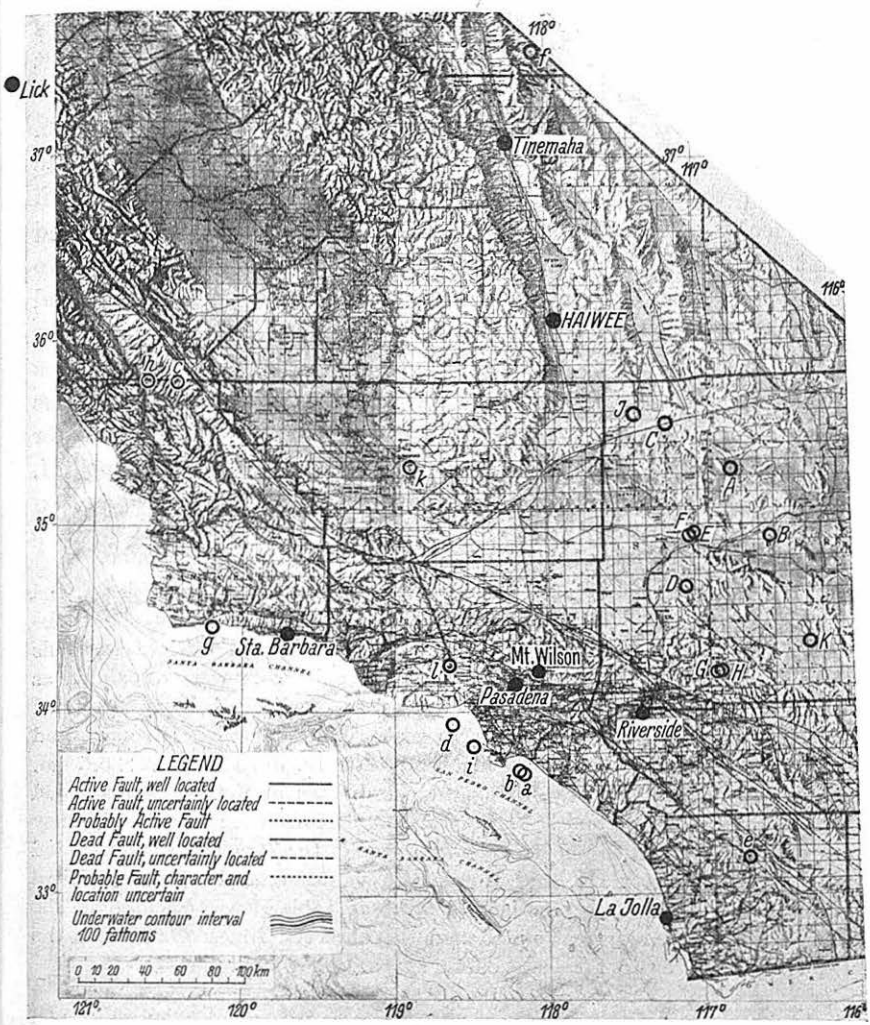

Fig. 1. Seismological stations (dots) and epicenters of earthquakes (lettered circles) in Southern California used in this paper.

contain all the larger shocks which have occurred in southern California since September, 1929. Shocks with an epicenter near the Mexican border, shocks northwest of Santa Barbara, and most shocks near La

Jolla and near Santa Barbara could not be used, because in these cases the other stations did not give sufficient data to use this method or because the intersections of the various lines mentioned above were very flat and not sharp. Finally, in some cases either the seismograms themselves or the time signals were disturbed and therefore sufficient data were not available.

The error created by the assumption of a velocity of 5.6 km./sec. for the $\overline{P}$-waves is not very great. Even if the two stations used were to show a difference of 10 seconds in the arrival of the waves and if the velocity of 5.6 km./sec. were in error by 0.2 km./sec., the second point would have been miscalculated by only 2 km.; and if the two points used were on opposite sides of the epicenter, the location found by the method would be in error by only 1 km.

Another difficulty arises from the fact that sometimes the $\overline{P}$-waves are not very sharp or not recognizable at all. In such cases the shocks were not used if the data from the other stations were insufficient for good results for the epicenters. All shocks finally used are given in table II. The position of the epicenters is shown in figure 1.

Table III. Calculation of epicenters and origin times.

The epicenters are indicated by the letters as given in table II, the abbreviations of the stations as given in table I. For every shock the first letter gives the station, the following numbers the minutes and seconds of beginning of the $\overline{P}$-phase. From these the epicenters were calculated as shown in the text. For example, in the case of shock A it was assumed that Haiwee was 1.7×5.6 km. nearer to the epicenter than Riverside and 4.4×5.6 km. nearer than Pasadena, and that La Jolla was 2.9×5.6 km. nearer than Santa Barbara. Using the coördinates of the epicenters found by these data, the distances of the various stations were calculated. They are given in km. Then the travel time curve of the $\overline{P}$-waves was calculated as shown in chapter III, and from these values and the time of arrival of the $\overline{P}$-waves the time of origin as given in table II was calculated. The differences between the calculated and the observed times of arrival of the $\overline{P}$-waves are given in the last column of the following table.

In each case the velocity of the $\overline{P}$-waves was then calculated, the best available epicenter being used. The values found varied within the limits of error, between 5.4 and 5.8 km./sec. But as we shall see, there was no reason to assume that this velocity depends upon the region passed over by the waves. On the other hand, the apparent velocity of the $\overline{P}$-waves is affected by the depth of focus, by the curvature of the earth and by the increase of velocity with depth. To

Table III. Calculation of epicenters and origin times.

Shock	Station	Time of arrival of $\overline{P}$ min sec.	Distance km.	$\overline{P}$ obs.—calc. sec. (first approximation)
A	H	07 25.3	140	—0.3
	R	27.0	146	+0.1
	P	30.7	173	—0.8
	J	48.1	263	+0.4
	S	51.0	278	+0.6
B	R	00 45.2	122	+0.3
	M	52.3	157	+1.2
	P	53.0	171	+0.1
	J	01 02.4	226	—1.0
	T	15.3	291	+0.2
	S	15.5	295	—0.3
C	M	12 46.0	163	+0.5
	R	46.8	170	+0.1
	P	47.4	176	—0.3
	T	51.0	194	+0.1
	S	13 02.1	257	—0.2
	J	08.6	292	0.0
D	M	52 40.8	103	+0.3
	P	42.6	117	—0.4
	H	54.6	181	+0.3
	J	56.8	197	—0.4
	S	53 05.8	245	—0.1
E	R	56 18.1	111	—0.2
	M	21.2	124	+0.5
	P	23.0	139	—0.3
	H	25.9	155	—0.1
F	R	53 19.2	109	—0.1
	P	24.4	137	+0.1
	H	27.6	155	0.0
	S	44.9	253	—0.2
	T	46.4	262	—0.3
G	R	24 42.6	48	—0.4
	M	53.4	106	+0.1
	P	55.0	118	—0.4
	H	25 15.4	230	0.0
	L	26 12.2	554	—0.2
H	R	34 12.5	48	+0.1
	M	22.8	106	—0.1
	P	24.9	118	—0.1

Table III (Continued).

Shock	Station	Time of arrival of $\overline{P}$ min. sec.	Distance km.	$\overline{P}$ obs.—calc. sec. (first approximation)
H	H	44.5	230	—0.5
	L	35 43.6	554	+1.6
J	M	34 37.6	166	+0.3
	P	39.2	178	—0.2
	T	39.9	179	+0.3
	R	40.3	179	+0.7
	S	51.9	250	—0.5
	J	35 01.2	302	—0.5
K	R	08 19.8	110	+1.2
	M	29.1	170	—0.2
	P	30.5	180	—0.6
	J	31.9	186	—0.3
	H	43.6	249	+0.3
	S	56.4	320	+0.3
a	P	39 34.0	54	+0.3
	R	39.0	86	—1.9
	J	47.9	123	+1.9
	S	53.4	165	0.0
	H	40 12.4	274	—0.6
	T	32.4	378	+0.9
b	R	23 53.5	86	—2.0
	J	24 00.5	123	—0.1
	S	08.5	165	+0.5
	T	47.4	378	+1.3
c	S	31 11.7	168	—0.8
	L	17.5	201	—0.8
	H	24.7	235	+0.3
	T	27.3	248	+0.5
	P	32.4	276	+0.7
	M	33.1	280	+0.6
	R	43.8	347	—0.7
d	P	40 44.9	46	+0.2
	S	56.5	113	—0.1
	R	57.1	117	—0.2
	J	41 07.7	176	0.0
	H	20.2	247	—0.3
	L	42 00.2	462	+1.3
	B	12.9	541	+0.2
e	J	26 00.4	557	+0.2

Table III (Continued).

Shock	Station	Time of arrival of $\overline{P}$ min. sec.	Distance km.	$\overline{P}$ obs.—calc. sec. (first approximation)
e	R	08.7	108	+0.5
	P	18.8	178	—0.7
	S	45.0	308	+1.1
	T	27 13.5	454	0.0
f	T	07 31.7	59	—0.9
	H	50.1	162	+0.3
	L	08 16.6	317	+1.0
	B	27.8	370	+0.7
	S	28.2	381	—0.8
	P	30.0	381	+1.0
	R	31.7	403	—1.3
g	S	09 04.0	45	+0.1
	P	29.4	188	+0.2
	R	43.8	267	+0.3
	H	45.5	279	—0.2
	J	54.0	324	+0.1
	L	57.3	346	—0.4
h	S	01 11.2	175	+0.3
	L	13.1	191	—0.7
	H	23.9	244	+0.5
	B	27.5	268	—0.2
	P	30.0	288	—0.3
	R	44.7	362	0.0
i	P	28 09.2	49	—0.1
	M	11.6	63	—0.1
	R	12.9	108	—1.5
	S	19.0	132	+0.3
	J	22.9	153	+0.5
	T	29 01.4	366	+0.7
k	S	27 04.0	124	0.0
	M	08.0	144	+0.4
	P	07.7	145	0.0
	R	17.3	204	—1.0
	T	18.0	205	—0.4
l	P	41 45.2	44	+0.1
	M	46.7	54	—0.1
	S	54.9	100	—0.1
	R	58.5	123	—0.7
	J	42 13.6	200	+0.8
	H	15.6	216	—0.1

Table IV.

Seismograms used for investigation of travel times. The first letter refers to the station (table I), the second to the shock (table II), the distance is given in km.

Pl	44	RE	111	Hf	162	JD	197	Pc	276	Pf	381
Sg	45	Sd	113	MC	163	Jl	200	SA	278	Rf	403
Pd	46	Rd	117	Sa	165	Lc	201	Hg	279	LJ	424
RG	48	PD	117	Sb	165	Rk	204	Mc	280	LC	442
RH	48	PG	117	MJ	166	Tk	205	Bc	281	Te	454
Pi	49	PH	117	Sc	168	Hl	216	Ph	288	Ld	462
Pa	54	RB	122	Me	169	JB	226	TB	291	Li	487
Pb	54	Ja	123	MK	170	HH	230	JC	292	LA	489
Ml	54	Rl	123	RC	170	HG	230	SB	295	BJ	500
Je	57	Jb	123	PB	171	Hc	235	JJ	302	Jf	525
Tf	59	ME	124	Pe	172	Hh	244	Se	308	LB	539
Mi	63	Sk	124	PA	173	Hd	247	Lf	317	Bd	541
Mb	64	Si	132	Sh	175	HK	249	SK	320	LG	554
Ra	86	PF	137	Jd	176	Tc	249	Jg	324	LH	554
Rb	86	PE	139	PJ	178	SJ	250	Td	346	Ue	555
Sl	100	HA	140	RJ	179	SF	253	Lg	346	UG	600
MD	103	Mk	144	TJ	179	Th	254	Rc	347	UH	600
MG	106	Pk	145	PK	180	SC	257	Rh	362	UB	606
MH	106	RA	146	HD	181	TF	262	Ti	366	BB	612
Ri	108	Ji	153	JK	186	JA	263	Bf	370	UA	640
Re	108	HE	155	Pg	188	Rg	267	Ta	378	BG	641
RF	109	HF	155	Lh	191	Bh	268	Tb	378	UC	687
RK	110	MB	157	TC	194	Ha	274	Sf	381	Ud	744

eliminate minor errors caused by these factors, the travel time curve of the $\overline{P}$-waves was constructed, the above-mentioned data (table III) being used; then the whole method was repeated in the case of each shock, but this time the velocity given by the travel time curve at the distance of each particular case was applied, instead of a velocity of 5.6 km./sec. The results obtained by using this better approximation did not differ very much from the previous ones, and when the whole method was again repeated the final results did not differ from those previously obtained.

Using the travel time curve of the $\overline{P}$-waves which we shall discuss later, we can now find also the origin time. The final values used in the calculation are given in table II.

With these epicenters and origin times the travel times for all measured phases were calculated. Table IV contains an enumeration of the seismograms used. Every record has a symbol of two letters the

first of which refers to the station (abbreviation in table I), the second to the shock (table II). For example HE means shock E (February 24, 1930), registered at Haiwee. The shocks marked by capitals occurred in the Mohave Desert or in the mountains surrounding it. Shocks from other regions (especially near the coast and from the Coast Ranges) are indicated by small letters.

III. The $\overline{P}$-waves.

On all seismograms listed in table IV the times of arrival of all marked impulses and of apparent changes in motion were measured. Since all stations in California have drum velocities corresponding to a length of one minute of 60 mm., so that 1 mm. in the seismogram equals 1 second, one tenth of a second can easily be read. Only at Tucson 1 mm. corresponds to 2 seconds. Besides, most of the seismograms were enlarged, usually two or three times, and all phases were read on these enlargements. The differences between all readings of the same phase were in general less than $^1/_4$ second in the case of $\overline{P}$-waves at distances less than 250 km., and less than $^1/_2$ second in most other cases. At very great distances the beginning of all phases is in general less precise. As mentioned before, the time of the southern

Table V.

Apparent velocity of the $\overline{P}$-waves. Shocks lettered as in table II. Velocity in km./sec.

Mohave shocks		Other shocks		
A 5.4	G 5.6	a 5.5	e 5.5	i 5.5
B 5.6	H 5.7	b 5.5	f 5.5	k 5.8
C 5.7	J 5.7	c 5.6	g 5.7	l 5.6
D 5.6	K 5.7	d 5.5	h 5.6	
F 5.6				

California stations relative to that at Pasadena station is in general correct within a few tenths of a second.

By using the epicenters given in table II and the corresponding distances for every shock, the apparent velocity of the $\overline{P}$-waves was calculated. For this purpose only waves from distances between 100 and 400 km. (as far as available) were used, because at distances of less than 100 km. the depth of focus might affect the result too much, while at distances over 400 km., and in some cases at still shorter distances, the $\overline{P}$-waves were rather indefinite or not recognizable at all. Table V shows the result. All values are between 5.4 and 5.8 km./sec.

Table VI.

Observed travel times of the $\overline{P}$-waves minus distance/5.55. The first column indicates the seismogram as in table IV, the second the distance Δ in km. and the third the difference $\overline{P}$ obs. $- \frac{\Delta}{5.55}$.

Pl	44	+ 0.5	Sh	175	+ 0.3	RJ	179	+ 0.7	JA	263	+ 0.4
Sg	45	+ 0.5	Jd	176	+ 0.0	PK	180	— 0.5	SA	278	+ 0.6
Pd	46	+ 0.6	Pg	188	+ 0.2	HD	181	+ 0.3	TB	291	+ 0.2
Pi	49	+ 0.3	Lh	191	— 0.7	SK	186	— 0.2	JC	292	0.0
Md	54	+ 0.2	Mean		+ 0.1	TC	194	+ 0.1	SB	295	— 1.1
Pa	54	+ 0.7	MD	103	+ 0.5	JD	197	— 0.4	Mean		— 0.2
Je	57	+ 0.6	MG	106	+ 0.3	Mean		+ 0.1	JJ	302	— 0.5
Tf	59	— 0.6	MH	106	+ 0.1	Jl	200	+ 0.8	Se	308	+ 1.0
Mi	63	+ 0.2	RF	109	+ 0.1	Lc	201	— 0.8	Lf	317	+ 1.0
Ra	86	— 0.6	RK	109	+ 1.4	Tk	205	— 0.4	JK	320	+ 0.2
Rb	86	+ 0.7	RE	111	0.0	Hl	216	— 0.1	Lg	346	— 0.5
RG	48	+ 0.0	PD	117	— 0.2	Hc	235	+ 0.3	Rc	347	— 0.8
RH	48	+ 0.3	PG	118	— 0.2	Hl	244	+ 0.5	Rh	362	0.0
Mean		+ 0.3	PH	118	+ 0.1	Hd	247	— 0.3	Ti	366	+ 0.8
Sl	100	+ 0.1	RB	122	+ 0.5	Tc	248	+ 0.5	Bf	370	+ 0.6
Re	108	+ 0.7	ME	124	+ 0.7	Rg	267	+ 0.3	Ta	378	+ 0.7
Ri	108	— 1.3	PF	137	+ 0.2	Bh	268	— 0.2	Tb	378	+ 1.1
Sd	113	+ 0.1	PE	139	— 0.2	Ha	274	— 0.6	Sf	381	— 1.0
Rd	117	0.0	HA	140	— 0.3	Pc	276	+ 0.7	Pf	381	+ 0.8
Rl	123	— 0.5	RA	146	+ 0.1	Hg	279	— 0.2	Rf	403	— 1.5
Ja	123	+ 2.1	HE	155	0.0	Mc	280	+ 0.6	LJ	424	— 0.6
Jb	123	+ 0.1	HF	155	+ 0.1	Ph	288	— 0.3	LC	442	— 2.1
Sk	124	+ 0.2	MB	157	+ 1.3	Mean		+ 0.1	Te	454	— 0.8
Si	132	+ 0.4	MC	163	+ 0.6	JB	226	— 1.0	Ld	462	+ 0.9
Mk	144	+ 0.5	MJ	166	+ 0.3	HG	230	0.0	Mean		— 0.0
Pk	145	+ 0.1	RC	170	+ 0.2	HH	230	— 0.5	BJ	500	— 2.2
Ji	153	+ 0.5	MK	170	— 0.1	SD	245	— 0.1	Bd	541	— 0.6
Hf	162	+ 0.4	PB	171	+ 0.1	HK	249	+ 0.2	LG	554	— 1.7
Sa	165	+ 0.1	PA	173	— 0.8	SJ	250	— 0.5	LH	554	+ 0.1
Sb	165	+ 0.6	PC	176	— 0.3	SF	253	— 0.2	Ue	555	— 1.4
Sc	168	— 0.7	PJ	178	— 0.2	Sc	257	— 0.2	UB	606	— 1.6
Pe	172	— 0.7	TJ	179	+ 0.3	TF	262	— 0.3	Mean		— 1.2

The mean value is somewhat less than 5.6 in the case of shocks near the coast and somewhat more than 5.6 km./sec. in the Mohave shocks. This small difference — if it exists at all — may be caused by sedimentary layers near some parts of the coast. In fact, some seismograms of shocks near the coast show at short distances (about 50 km.) a small wave preceding the sharp beginning by a very few tenths of a second,

which indicates a layer that does not exist more distant from the coast. The seismograms available are not sufficient to furnish details. On the other hand, the apparent velocity of the $\overline{P}$-waves is generally somewhat higher at great distances, due to the earth's curvature and the increase of velocity with depth. In order to find this effect, as well as the effect of the depth of focus, the difference between the observed travel times (time of arrival of $\overline{P}$ minus calculated time of origin) and the value distance (km.) divided by 5.55 was calculated. It was found, as expected, that at short distances the waves arrived too late, and at long distances too early, as compared with the given constant velocity (fig. 7). A mean curve was drawn through the observed differences, and using the travel times corrected by this curve, the origin times of the various shocks were calculated again. The corrections were in general less than $^1/_2$ second. No correction of the epicenter seemed necessary. The origin times found by this procedure are given in table II. Then the travel times of the $\overline{P}$-waves were calculated again. Their deviations from the value distance/5.55 are shown in table VI. For distances between 100 and 300 km. the Mohave shocks were treated separately from the other shocks. It will be recognized that between 100 and 200 km. there is no difference. At longer distances the $\overline{P}$-waves from Mohave shocks arrived some tenths of a second sooner than from the others, the difference, however, being within the limits of error.

The principal result of table VI is that at distances between 44 and 86 km. the waves arrived in general 0.3 seconds earlier than would correspond to an apparent velocity of 5.55 km./sec. Between 100 and 200 km. this difference decreased to a mean of 0.1 second; in the following interval the difference was practically zero; at distances over 400 km. the difference was nearly always negative and the mean passed below —1.0 seconds between 500 and 600 km. The values themselves are not very precise at such great distances, as the beginning of the $\overline{P}$-waves becomes less distinct at distances over 400 km. At distances over 606 km. the $\overline{P}$-wave disappeared entirely. The most distant wave of this kind corresponds to the wave which at its deepest point touches the second layer. It is therefore not possible to calculate any absorption coefficient for the granitic layer, due to the fact that no $\overline{P}$-waves are recognizable at large distances. Neither can the depth of this second layer be found from these data, as the curvature of the wave paths caused by the increase of velocity with depth is not known well enough for such calculation.

The most probable values of the travel times of $\overline{P}$ in southern California are given in table VII where, besides, the observed differences between these times and the times corresponding to an apparent velocity of 5.55 km./sec. are compared with the corresponding values of the travel time curves of A. Mohorovičić for different depths of focus (13). It can be seen that our curve, far within the limits of error, has the same shape as the curve of Mohorovičić for a depth of focus of 10 km., which was interpolated from two curves given in table VII.

IV. P_n and P_x.

Beginning at a distance of somewhat over 100 km. the first waves of the seismograms are the normal longitudinal waves. Since only a very small amount of energy reaches the surface of the earth in this way, as pointed out in previous investigations, these P_n-waves are very small. The travel times (calculated from the observed times of arrival of P_n and the origin times as given in table II) are shown in table VIII. To find an analytic expression for the travel time curve of these waves (and also in the case of all following waves) a straight line was assumed as a first approximation, which fitted some of the observations at very short distances and some at very long distances. The differences between this line and the observed points were calculated, then from these the mean difference for each interval of 100 km., and with the values thus found a second approximation was tried. Where necessary, the whole procedure was repeated. In each case (except $\overline{P}$) it was possible to fit the data assuming that the travel time curve was a straight line. The best approximation to the travel time of P_n was given by $5.8 + \frac{\Delta}{7.94}$.

Table VII. Travel times t of $\overline{P}$-waves.

Δ km.	Travel times minus (distance/5.55) according to Mohorovičić h=0 km.	10 km. (interpol.)	25 km.	S. California obs. (table VI)	Probable values of t, Southern California
0	0.0	1.8	4.5	—	—
50	0.1	0.4	0.9	0.4	9.4
100	0.1	0.2	0.4	0.2	18.2
200	0.1	0.0	—0.1	0.0	36.0
300	0.0	—0.2	—0.4	—0.1	53.9
400	—0.3	—0.5	—0.8	—0.2	71.9
500	—0.5	—0.7	—1.1	—0.5	89.6
600	—0.8	—1.2	—1.8	(—1.5)	(106.6)

Table VIII.

Observed travel times t of P_n and differences D of these values minus $\left(5.8 + \frac{\Delta}{7.94}\right)$.

List of diagrams as in table IV.

Diagr.	Δ	t	D	Diagr.	Δ	t	D
Sd	113	20.0	0.0	TC	194	31.3	+1.0
Rd	117	20.7	+ 0.1	Lc	201	31.2	0.0
PD	117	20.6	0.0	HG	230	34.5	— 0.3
PG	118	20.3	— 0.4	HH	230	35.2	+ 0.6
PH	118	20.6	— 0.1	Hc	235	36.1	+ 0.7
Jb	123	20.7	— 0.6	Hh	244	35.7	— 0.9
Sk	124	21.8	+ 0.4	Hd	247	37.5	+ 0.6
ME	124	21.4	0.0	Tc	248	37.5	+ 0.4
Si	132	23.0	+ 0.6	Bh	268	38.1	— 1.5
PF	137	23.1	0.0	Ha	274	38.8	— 1.5
PE	139	23.7	+ 0.4	Pc	276	41.1	+ 0.5
Ji	153	26.1	+ 1.0	Hg	279	42.1	+ 1.1
HE	155	25.4	+ 0.1	MC	280	40.9	— 0.2
HF	155	26.0	+ 0.7	Ph	288	41.3	— 0.8
MB	157	25.4	— 0.2	TB	291	42.7	+ 0.2
Sa	165	26.5	— 0.1	Rc	347	48.9	— 0.6
Sb	165	26.1	— 0.5	Ta	378	52.6	— 0.8
Sc	168	27.1	+ 0.1	Ld	462	64.5	+ 0.5
RC	170	28.4	+ 1.2	LB	539	73.8	+ 0.1
Sh	175	27.4	— 0.4	LG	554	76	— 0.4
Pg	188	29.5	0.0	LH	554	75	+ 0.6
Lh	191	29.5	— 0.4				

Table IX.

Travel times of P_n and difference in the travel times of $\overline{P}$ and P_n according to various investigations.

Δ km.	Travel time S. Calif. Gutenberg	Difference $\overline{P}-P_n$					
		S. Calif. Gutenberg	S. Germ. Gutenberg	Schwadorf Conrad	Tauern Conrad	Kulpatal Mohorovičić	Tajima Matuzawa
100	(18.4)	—0.2	—	—	—	—	—
200	31.0	5.0	2.9	2.2	2.8	1.6	4.0
300	43.6	10.3	8.7	8.3	8.0	7.0	8.2
400	56.2	15.7	13.8	12.8	12.9	12.0	12.5
500	68.8	20.8	18.6	18.6	17.6	16.6	16.7
600	81.4	25.2	22.8	22.7	22.2	—	20.3

Caucasus (N. W. Rajko): $\Delta = 300$ km., $\overline{P}-P_n = 8.1$ sec. (average).

In other regions the following values had been found:
Schwadorf (Austria) by CONRAD (assuming a depth of focus of 28 km.)

$$9 + \frac{\Delta}{8.12}$$

Tauern (Alps) by CONRAD

$$8\,\tfrac{3}{4} + \frac{\Delta}{7.83}$$

Kulpatal (Jugoslavia) by A. MOHOROVIČIĆ

$$9\,\tfrac{1}{2} + \frac{\Delta}{7.9}$$

South Germany by GUTENBERG

$$9\,\tfrac{1}{2} + \frac{\Delta}{8.2}$$

The first, constant term of all these values is rather uncertain, as it depends upon the supposed depth of focus. Nevertheless it is quite evident that in our region the P_n-waves arrive earlier than in the other regions considered above. Values between those given for California and the others cited above seem to have occurred in England, as found by JEFFREYS, but his data were not sufficient to calculate a definite depth of focus.

To avoid the error caused by the uncertain depth of focus, in table IX the time differences between $\overline{P}$ and P_n are given for California and some other regions. From these data it is quite evident that the P_n-waves actually arrive earlier in California than in any other country considered in table IX. We shall consider these results when dealing with the thickness of the layers and the depth of focus.

In figure 2 the time difference $\overline{P}$—P_n is plotted against the distance for the shocks available. The distance, at which the two travel time curves intersect, is approximately 150 km. in Europe but only somewhat over 100 km. in California.

When investigating the Schwadorf (Austria) earthquake, V. CONRAD (4) found that there was a phase a few seconds after the P_n-wave. He called it P_x and stated that in the travel time curves of the South German shocks in 1911 and 1913 corresponding travel times had also been found by GUTENBERG. In many of our seismograms this P_x-wave is very distinct at distances over 200 km. As can be seen from the curves reproduced in figure 11, the wave is in general larger than P_n, and in some cases at very great distances the P_n-wave undoubtedly

was too small to be found, while the P_x-wave could be seen distinctly. Similar results have been found by CONRAD.

In table X the observed travel times of the P_x-wave and the observed time differences $P_x - P_n$ are given. The travel time of P_x cor-

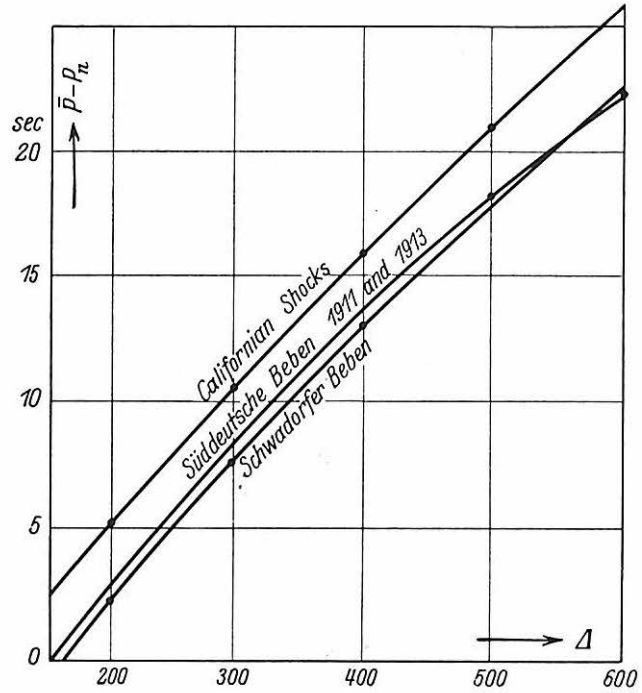

Fig. 2. Travel-time difference $\bar{P} - P_n$ in different countries.

responds within the limits of error, as shown in the last column of table X, to the equation $t = 4.9 + \frac{\Delta}{7.60}$

where Δ (as throughout this investigation) is measured in km. and t in seconds. CONRAD's corresponding equation for Schwadorf, Austria (if we assume again a focal depth of 28 km.) is

$$t = 9.7 + \frac{\Delta}{7.87}.$$

The time difference $P_x - P_n$ is given by $-0.9 + 0.0056\,\Delta$ in California and by $0.7 + 0.004\,\Delta$, according to CONRAD, for the Schwadorf quake.

Table XI shows the mean travel times of the P_x-wave in California, the mean time differences $P_x - P_n$ and the corresponding values found by CONRAD.

V. Other waves between P_n and $\overline{P}$.

Between P_n and $\overline{P}$ there are some other well-marked phases. They can be divided into two classes: waves of the first class are well marked at short distances. They are visible when their travel times are less than the travel times of $\overline{P}$. At shorter distances they can sometimes be seen beyond $\overline{P}$, but the strong motions caused by $\overline{P}$ generally prevent a precise beginning of these phases in the records. They decrease with increasing distance and disappear at distances of a few hundred km., similar to $\overline{P}$. From every point of view, it seems probable that these waves are longitudinal waves through deeper layers. Only in a few cases were seismograms of a vertical component available, and they all show that these waves have a rather large vertical component (fig. 8).

Table X.

Travel times t of P_x, observed time differences $P_x - P_n$ and difference observed—calculated travel times.

Shock	Dist.	t	$P_x - P_n$	$t - (4.9 + \Delta/7.6)$
Hc	235	36.7	0.6	+ 1.1
Hd	247	38.0	0.5	— 0.4
Tc	248	37.8	0.3	— 0.7
Th	254	?	0.8	?
Mc	280	40.4	0.5	— 1.4
Ph	288	42.1	0.8	— 0.7
TB	291	43.7	1.0	+ 0.5
SB	295	44.2	?	+ 0.5
Lg	346	50.9	1.4	+ 0.5
Bf	370	53.7	?	+ 0.1
Pf	381	54.8	?	— 0.2
Te	454	64.2	?	— 0.4
Ld	462	66.8	2.3	+ 1.1
LB	539	75.6	1.8	+ 0.7

Table XI.

Mean travel times t of P_x, mean observed values $P_x - P_n$ and corresponding values found by V. CONRAD with respect to the Schwadorf (Austria)-shock.

Distance km.	t sec.	$P_x - P_n$ (sec.) California	Austria
200	31.2	0.2	(1.4)
300	44.4	0.8	1.8
400	57.5	1.4	2.2
500	70.7	1.9	2.6

Table XII.

Travel times of P_m and P_y in California, differences as against the travel time of P_n and travel time differences $P^*—P_n$ in other regions.

Distance km.	Travel time		California		Schwadorf $P^*—P_n$ sec. CONRAD	Europe $P^*—P_n$ sec. GUTENBERG
	P_m sec.	P_y sec.	$P_m—P_n$ sec.	$P_y—P_n$ sec.		
100	(18.5)	17.8	(0.1)	—	—	—
200	33.2	34.4	2.2	3.4	—	1
300	47.8	50.9	4.2	7.3	4.0	4
400	62.5	67.5	6.3	11.3	7.2	7
500	77.1	84.0	8.3	15.2	10.4	10
600	91.8	100.5	10.4	19.1	13.6	12

Table XIII.

Travel times of a, b and c in Southern California.

Distance km.	Travel time of		
	a	b	c
250	38.2	42.4	43.5
300	45.3	50.0	51.8
400	59.4	65.3	68.7
500	73.4	80.5	85.5
600	87.5	95.8	102.4
700	101.6	111.1	119.3

The second class of waves between P_n and $\overline{P}$ is noticed especially at greater distances. It therefore is quite probable that they are not caused by a layer but by some other factor.

In the seismograms of the California shocks two kinds of waves of the first class could be found — they were marked P_m and P_y — and three kinds of the second class — they were called a, b and c. The time differences of all these waves compared with P_n are plotted in figure 3.

As stated before, the only well-marked waves at distances less than 300 km. are P_m and P_y. In figure 4 the mean time differences of these two waves compared with P_n are plotted, together with the observed time differences of $P^* — P_n$ in Europe. It will be noticed that P_m seems to correspond to P^* in Europe, but there are also some points of P^* or other phases (without symbol by the investigator) corresponding to our P_y.

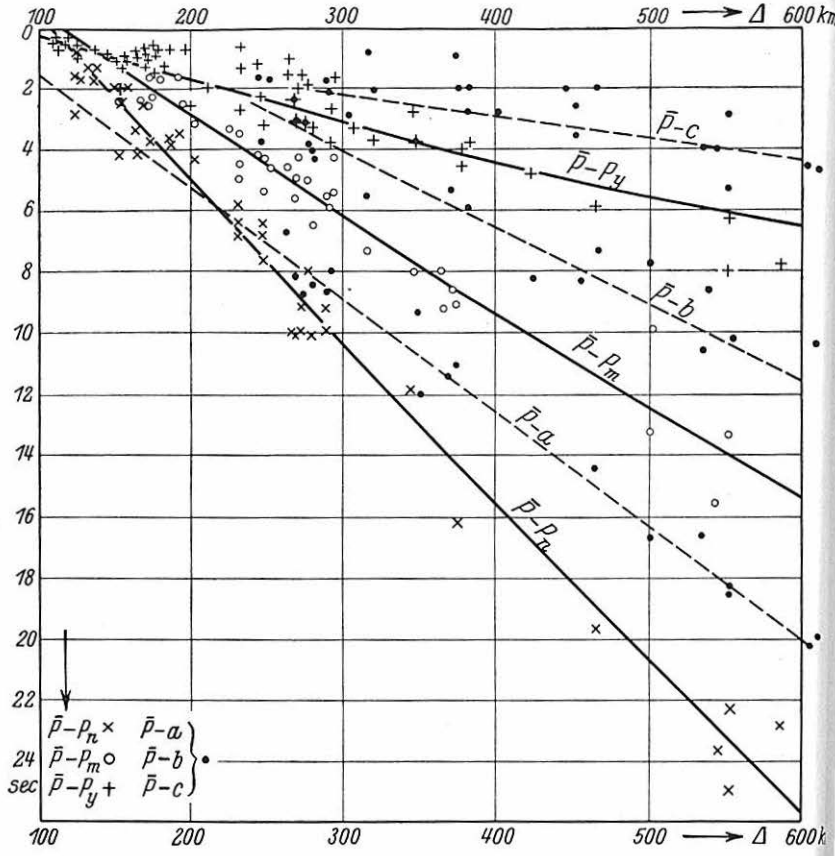

Fig. 3. Differences in travel-times between $\bar{P}$ and other waves arriving earlier. Southern California.

The equations of the travel times of these two waves are

$$P_m: \qquad t = 3.9 + \frac{\Delta}{6.83}$$

$$P_y: \qquad t = 1.3 + \frac{\Delta}{6.05},$$

so that the apparent velocities are 6.83 and 6.05 km./sec., respectively. The corresponding values found in other countries for P^* are

South Germany 1911	GUTENBERG	7.1 km./sec.
Tauern (Alps)	CONRAD	6.29
Jersey (England)	JEFFREYS	6.3
Herfordshire (England)	,,	6.3

Schwadorf (Austria)	CONRAD	6.47 km./sec.
South Germany (mean)	GUTENBERG	6.5
North Germany (explosion)	BROCKAMP	6.9 (upper layer 5.9—6.1)
Japan, different investigations		6—$6^1/_4$.

From a comparison of these values it seems quite evident that some of them correspond to our values of P_m and others to P_y. In some instances the two waves may have been treated jointly, and a mean travel time curve may have been found.

The velocities found in North Germany by explosions (2) correspond also very well to the values found in California for P_m and P_y. There-

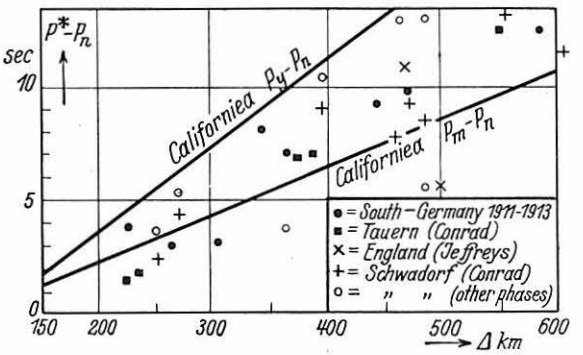

Fig. 4. Observed differences in travel-times $P^*—P_n$ in Europe, and mean observed curves $P_y—P_n$ and $P_m—P_n$ in California.

fore it seems quite probable that in North Germany the upper layer, with a velocity of 5.5 km./sec., is entirely absent and that the $\bar{P}$ there corresponds to our P_y, and the wave following $\bar{P}$ there to our P_m.

In table XII the travel times of P_m and P_y and their differences from P_n are given, as well as the differences $P^*—P_n$ as found in Europe.

The second class of phases between $\bar{P}$ and P_n is especially well marked at long distances. In figure 3 they are marked by dots. Regarding this figure it sometimes seems rather arbitrary to decide whether we have a wave of this kind or one of the waves mentioned before. But the use of seismograms generally makes it possible to determine with certainty the kind of waves occurring in a given case. At short distances there are in general only P_m and P_y-waves, at very long distances only the other waves are conspicuous. Three kinds of such waves were marked. They were called a, b and c. Their travel

times t could be expressed by the following formulas (the corresponding straight lines are drawn in figure 3):

a) $$t = 3.0 + \frac{\Delta}{7.10}$$

b) $$t = 4.3 + \frac{\Delta}{6.56}$$

c) $$t = 1.4 + \frac{\Delta}{5.94}$$

The most striking of these waves is a. Its travel times correspond very well to those found by STONELEY (15) in many shocks, especially in Europe, with travel times given by

$$t = 2.5 + \frac{\Delta}{7.0}.$$

In our case as well as in shocks considered by STONELEY all observations relate to distances of a few 100 km. STONELEY had no seismographic observations from distances less than 300 km. But our 16 seismograms relating to distances between 86 and 117 km. show distinctly that the straight line given by equation a can not be traced back nearer than 120 km., as the a-wave must arrive there $1^1/_2$—2 seconds before the first P-waves arrive, but undoubtedly no movement can be found there. The wave found by STONELEY in European seismograms must also be the first one at these distances, if his equation is correct. But in the case of the South German shock also no wave of this kind was registered, although the seismograms show very large amplitudes at these distances. From this it must be concluded that the a-wave either begins at a greater distance, or its travel time curve is not a straight line. In either case the wave can not be a longitudinal wave that passed a deeper layer, but it must have been caused in some other way, as yet unknown to us. The same holds in the case of the b- and c-waves, which also are very small at short distances, but increase slightly with distance. These two waves are, moreover, less definite.

VI. *S*-waves and surface waves.

As stated before, it is sometimes rather difficult to decide to which kind of waves a certain phase in the region of the longitudinal waves belongs. This difficulty is even greater in the region of the S-waves, on account of the greater number of reflected and refracted waves as well as surface waves there. According to the theory given by NAKANO,

we must, at short distances, observe the surface shear-wave (Q-wave, Love wave) earlier than the $\overline{S}$-wave. The distance at which the two travel time curves intersect, depends upon the depth of focus (8, 9). In any case the travel time curves of these two waves must be very close together. Assuming a 12 km. depth of focus and the observed velocities of longitudinal and transversal waves, we obtain theoretically the following differences between the arrival of the Q-waves and the $\overline{S}$-waves:

Distance	50	100	200	300	400	500	600 km.
Q—$\overline{S}$	—0.8	—0.3	+0.1	+0.5	+1.1	+1.7	+2.5 sec.

Table XIV.

Observed travel times of the Q-($\overline{S}$-)waves and differences $Q - \Delta/3.23$. Column 1 indicates the diagram as in table IV, Col. 2 the distance in km., Col. 3 the travel time and Col. 4 the difference observed minus calculated time.

Pl	44	14.2	+0.6	PE	139	42.6	—0.4	Tc	248	78.4	+1.6
Sg	45	14.2	+0.3	HA	140	44.3	+0.9	SJ	250	78.6	+1.2
Pd	46	14.0	—0.2	RA	146	44.5	—0.7	SF	253	78.7	+0.4
RG	48	15.8	+0.9	HE	155	48.3	+0.3	SC	257	79.2	—0.4
RH	48	16.0	+1.1	HF	155	48.5	+0.5	TF	262	80.9	—0.2
Pi	49	14.5	—0.7	Mc	163	51.1	+0.6	JA	263	82.0	+0.6
Pb	54	15.6	—1.0	Sa	165	51.3	+0.2	Bh	268	83.9	+0.9
Ml	54	16.1	—0.5	Sb	165	51.7	+0.7	Ha	274	84.1	—0.7
Je	57	17.0	—0.5	MK	170	51.3	—1.3	SA	278	86.1	+0.0
Tf	59	17.4	—0.9	Rc	170	52.3	—0.4	Ph	288	90.2	+0.9
Mi	63	20.3	+0.8	Pe	172	53.1	—0.2	JJ	302	93.4	+0.2
Ra	86	26.4	—0.2	PA	173	54.1	+0.5	Se	308	95.3	—0.1
Rb	86	26.3	—0.3	Sh	175	54.7	+0.5	Lf	317	99.0	+0.8
Sl	100	31.5	+0.5	Jd	176	54.4	—0.1	SK	320	98.2	—1.0
MD	103	32.9	+1.0	PJ	178	55.3	+0.1	Rc	347	107.7	+0.3
MG	106	33.8	+1.0	TJ	179	54.4	—0.9	Bf	370	114.7	+0.1
MH	106	32.7	—0.1	RJ	179	54.1	—1.3	Ta	378	115.8	—1.2
Re	108	34.5	+1.0	PK	180	54.7	—1.0	Tb	378	116.8	—0.2
RF	109	33.3	—0.5	HD	181	54.9	—1.1	Pf	381	117.3	—0.6
RK	110	34.6	+0.5	Lh	191	59.1	0.0	Jl	424	131.2	+0.0
RE	111	34.3	—0.1	Tc	194	61.2	+1.0	Te	454	138.9	—1.8
Rd	117	36.1	—0.1	JD	197	60.2	—0.8	Ld	462	144.6	+1.6
Pd	117	35.1	—1.1	Jl	200	63.3	+1.4	Li	487	150.5	—0.3
Pg	118	36.9	+0.3	Lc	201	61.9	—0.3	LA	489	150.9	—0.5
PH	118	35.7	—0.9	Ll	216	68.8	+1.9	LB	539	166.6	—0.4
Ja	123	39.0	+0.9	HH	230	71.4	+0.1	LG	554	771	—0.7
Rl	123	38.9	+0.8	Hc	235	72.2	—0.5	Ue	554	169	—2.7
Me	124	38.0	—0.4	Hh	244	74.5	—1.0	UH	600	185	—0.9
Sk	124	38.7	+0.3	SD	245	74.8	—1.1	BB	612	190.7	+0.9
Si	132	40.4	—0.5	HD	247	76.5	0.0	Ud	744	229	—1.2

The observed travel times of the corresponding wave are given in table XIV. The observations fit very well the straight line given by $t = \Delta/3.23$. This apparent (or in this case perhaps true) velocity corresponds very well with the value 3.21 km./sec., found by H. O. Wood and C. Richter (16) for transversal waves in California that were caused by blasts. The fact that the difference between calculated and observed values, also shown in table XIV, shows no change with distance (as it does in the case of the $\bar{P}$-waves) favors the assumption that we have observed Q-waves. This would not be impossible, as at distances shorter than 200 km. the Q-wave must precede the $\bar{S}$-wave by a few tenths of a second. As stated before, at a distance between 200 and 300 km. both waves arrive at the same time within $^1/_2$ second, and at greater distances the $\bar{S}$-wave may decrease like the $\bar{P}$-wave, so that only the Q-wave can be observed there. However, this problem

Table XV.

Observed time differences $S_x - S_n$.

Seismogram	Distance	$S_x - S_n$
JA	263	1.8
Bh	268	2.5
Ph	288	1.7
TB	291	2.4
JC	292	1.7
Rc	347	1.9
Ld	462	3.6
UH	600	3
UB	606	4

Table XVI.

Mean travel times of S-waves and surface waves.

Distance	Travel time of					
km.	S_n	S_x	S_m	S_y	$\bar{S}\,(Q)$	R
50	—	—	—	—	15.5	16.8
100	33.1	—	31.7	31.0	31.0	33.5
200	55.5	56.0	59.0	60.5	61.9	67.1
300	78.0	79.6	86.3	90.0	92.8	100.7
400	100.5	103.2	113.7	119.5	123.8	134.2
500	122.9	126.7	141.1	149.0	154.7	167.8
600	145.5	150.3	168.4	178.5	185.6	201.4
700	?	?	?	208.0	216.5	234.9

requires further investigation. In Europe the two waves might be found separately, due to greater depths of focus causing a greater difference between the arrival of the Q-waves and the $\overline{S}$-waves (8).

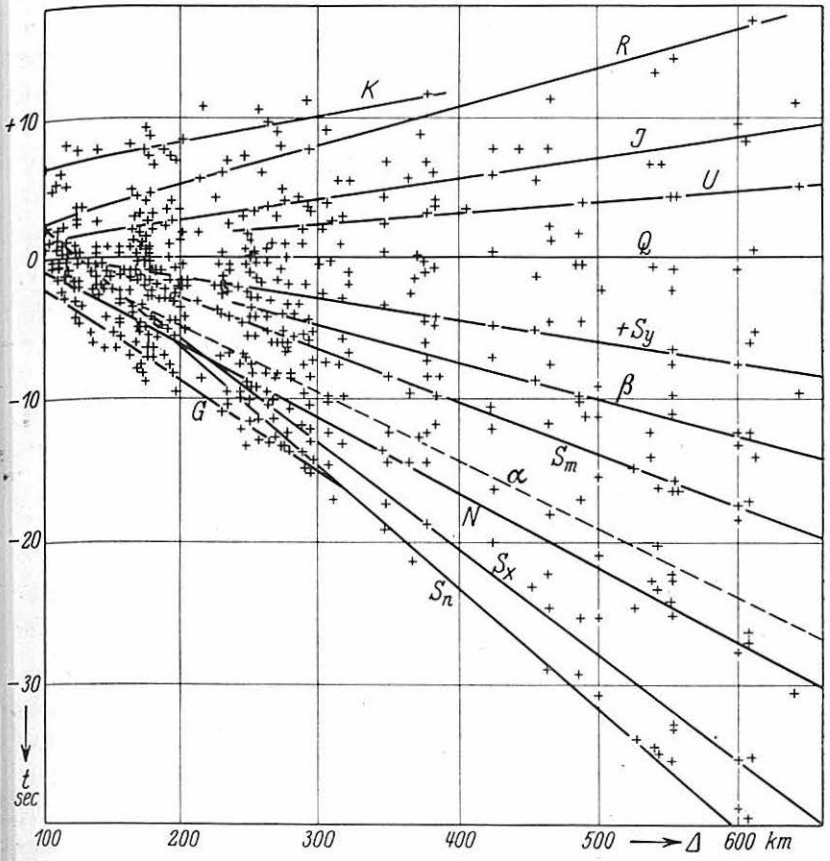

Fig. 5. Differences in travel-times of various waves and the surface shear wave Q.

Some other remarkable waves have been found, with similar properties to those of the corresponding P-waves; they are very large at short distances and decrease at distances of some hundreds of km. The differences of their travel times as compared with the travel times of the Q- (or $\overline{S}$-) wave are plotted in figure 5 against the distance, together with the travel time differences of other waves. Here, even more than in the case of the P-waves, the travel time curves are more definite

than shown in the figure, as the different phases have entirely different amplitudes and besides they sometimes differ in their general aspect.

The following formulas have been found for the travel times:

$$S_n \qquad t = 10.6 + \frac{\Delta}{4.45}$$

$$S_x \qquad t = 8.8 + \frac{\Delta}{4.24}$$

$$S_y \qquad t = 4.4 + \frac{\Delta}{3.66}$$

$$S_m \qquad t = 1.5 + \frac{\Delta}{3.39}$$

The observed time differences between S_x and S_n are given in table XV.

With respect to the Schwadorf quake CONRAD (4) found the following travel times (assuming a focal depth of 28 km.):

$$S_x \qquad t = 5.8 + \frac{\Delta}{4.32}$$

$$S^* \qquad t = 1.7 + \frac{\Delta}{3.57}$$

$$\overline{S}\,(iL) \qquad t = 0.7 + \frac{\Delta}{3.39}$$

The apparent velocities found by JEFFREYS (10) for two English earthquakes and by MOURANT (14) for earthquakes in the English Channel are

$$S\ 4.35 \qquad S^*\ 3.7 \qquad Sg\ 3.3.$$

Finally GUTENBERG (7) found, in the case of the South German earthquakes of 1911 and 1913, 3.75 as apparent velocity of iL (S^*?). All travel times of CONRAD are noticeably smaller than the corresponding values in California. Aside from this the two S_x-curves and JEFFREYS' value for S correspond very well. Perhaps in some cases he had S_n. Furthermore, there is good agreement between S_y in California and S^* in Europe, and finally CONRAD's $\overline{S}$-curve and our S_m-curve are nearly the same. In fact, in California also S_m has very often the largest amplitudes on the seismogram, and very often it has been marked as the beginning of the maxima. As stated by CONRAD, it was found that in most cases the wave of near earthquakes, called "iL" in the first investigation, belongs to different phases in different instances, sometimes to the G-wave, which we shall consider afterwards and which arrives earlier than any S-wave, sometimes to S_x, quite often to S_y or S_m, sometimes to the true iL and sometimes even to a later phase.

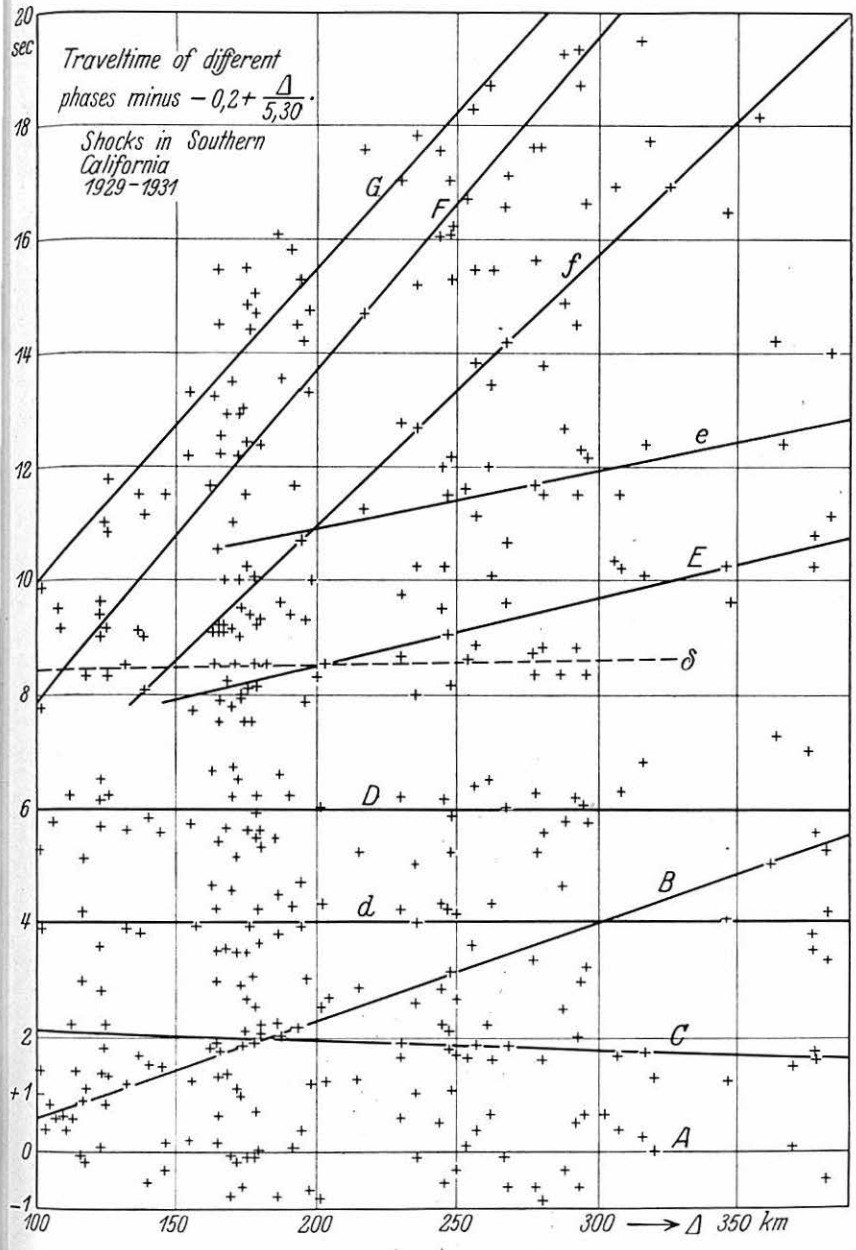
20
sec
Traveltime of different
phases minus $-0{,}2+\frac{\Delta}{5{,}30}$.
Shocks in Southern
California
1929–1931
18
16
14
12
10
8
6
4
2
+1
0
−1
G
F
f
e
E
δ
D
d
B
C
A
100
150
200
250
300
Δ 350 km

Fig. 6.

One of these later phases seems to be the RAYLEIGH wave (R), but the material was not sufficient to prove this. The travel time of this curve is given by $t = \Delta/2.98$.

VII. Other waves.

We know that if a longitudinal or a transversal wave touches a surface between two different layers, it divides into 4 waves. Since there are several surfaces of this kind within the upper 40 km. of the earth's shell, we must expect a large number of reflected and refracted waves. If we knew more about the ratio of the energy in the different waves, we could select waves with probably small energy and waves with larger energy. But calculations have been made only in a very few cases. In general the greatest amount of energy is propagated with the refracted wave of the same kind as the incident wave; in general a more or less considerable amount of energy is found in the reflected wave of the same kind. This energy is especially large, if the refracted wave does not exist beyond its critical angle of incidence. The waves of the other kind (transversal waves, if a longitudinal wave is incident) are in general small according to the theory.

Besides these different kinds of waves we have to expect surface waves in all layers. The general theory of these waves has been given by ULLER, but no special calculations have been carried out to date.

Evidently the a-, b- and c-waves discussed heretofore belong to one or the other kind of waves mentioned above. In that part of the seismograms following the P-waves there are some very distinct though in general not very large phases. Figure 6 shows the observations and the probable travel time curves for such waves at distances between 100 and 400 km. and between $\overline{P}$ and S_n, figure 7 at distances less than 100 km. In figure 6 the zero-line is given by the probable travel time of the A-wave. The C-, d- and D-wave and perhaps another δ-wave seem to have travel time curves nearly parallel to the curve of the A-wave. Some of these phases are quite conspicuous in the seismograms (fig. 8—11). Other waves of this kind are marked in figure 5. The travel times of these waves are given in table XVII.

The different travel time curves can be given by the following equations:

A. In general well marked; amplitudes often larger than the amplitudes of P, which it follows within a very few seconds

$$t = -0.2 + \frac{\Delta}{5.3}$$

B. Often well marked $t = -1.2 + \frac{\Delta}{4.87}$

C. To be found at all distances $t = 2.2 + \frac{\Delta}{5.36}$

d. Follows C after nearly 2 seconds $t = 3.8 + \frac{\Delta}{5.3}$

D. Again two seconds later $t = 5.8 + \frac{\Delta}{5.3}$

E. In general considerable $t = 6.0 + \frac{\Delta}{5.0}$

e. Only at distancees betwen 200 and 500 km., in general not very large $t = 9.0 + \frac{\Delta}{5.06}$

f. Only at distances over 200 km., but sometimes rather sharp there $t = 1.9 + \frac{\Delta}{4.28}$.

This wave is perhaps identical with the one found by CONRAD in the Schwadorf quake to which he had given the sign "*d*". The travel times there were given by $t = -0.6 + \frac{\Delta}{4.19}$. Also, in the seismograms of the South German shocks in 1911 and 1913 there are some waves with similar travel times.

g. This wave was considerable only at distances over 400 km. Its travel times can be given by

$$t = 14 + \frac{\Delta}{5.0}.$$

Its travel time curve is nearly parallel to the curves of E and e.

F. Sometimes rather sharp

$$t = 1.8 + \frac{\Delta}{4.04}.$$

G. Very often considerable at small distances, where it looks like "*eL*". At distances over 300 km. it arrives after the first *S*-waves and therefore can not be found. Its travel times are given by $t = 4.3 + \frac{\Delta}{4.1}$.

N. At short distances very well marked. Near 200 km. it has nearly the same travel times as S_n and S_x, but at longer distances it is again visible. Perhaps it corresponds to the α-wave found

by CONRAD in the Schwadorf quake, with travel times given by $t = 2.9 + \Delta/3.81$. The travel times of N are given by

$$t = 4.6 + \frac{\Delta}{3.9}.$$

α. Often well marked at long distances. $t = 4.5 + \frac{\Delta}{3.80}$.

β. One of the largest waves at great distances. Its beginning is very often extremely well marked. Perhaps α and β correspond to the a- and b-waves in the region of the longitudinal waves.

U. Sometimes considerable at great distances

$$t = \frac{\Delta}{3.16}.$$

J. Quite often very sharp with large amplitudes

$$t = -0.2 + \frac{\Delta}{3.09}.$$

K. Occurs only at distances less than 300 km., but is sometimes very sharp with large amplitudes

$$t = 4.5 + \frac{\Delta}{3.05}.$$

Table XVII.
Travel times of different phases.

Distance	Travel time of phase								
km.	A	B	C	d	D	E	e	f	g
50	9.2	—	11.5	13.2	15.2	—	—	—	—
100	18.7	19.3	20.9	22.7	24.7	26.0	—	—	—
200	37.6	39.9	39.6	41.6	43.6	46.0	48.5	48.6	—
300	56.4	60.4	58.2	60.4	62.4	66.0	68.3	71.9	—
400	75.3	81.0	76.9	79.3	81.3	86.0	88.1	95.2	94.0
500	94.2	101.5	95.6	98.2	100.2	106.0	107.9	118.6	114.0
600	113.1	122.0	114.2	117.1	119.1	126.0	127.7	141.9	134.0
700	—	—	—	—	—	146.0	—	—	154.0

	F	G	N	α	β	U	J	K
50	—	—	17.4	—	—	—	—	20.9
100	26.6	28.7	30.2	—	—	—	32.2	37.3
200	51.3	53.1	55.9	57.1	—	—	54.5	70.1
300	76.0	77.4	81.5	83.4	87.9	94.9	96.9	102.9
400	100.8	—	107.1	109.7	116.5	126.5	129.2	—
500	—	—	132.8	136.1	145.2	158.2	161.6	—
600	—	—	158.4	162.4	173.8	189.9	194.0	—
700	—	—	—	188.7	202.4	221.4	226.3	—

Table XVIII.

Calculated depths of focus. a) By use of macroseismic data and the formula of GASSMANN (I = maximum intensity, r = radius of the shaken area, h = depth of focus).

Shock	I	r	h
a	4	20	7
b	5	40	7
c	4	60	22
d	7	150	15
e	4	40	15
g	5	70	14
h	4	50	18
i	6	50	5
G	7	250	9
Mean	—	—	12

b) By use of the travel times of $\overline{P}$.

Shock	Distance	$\overline{P}$—(Δ/5.55)	h
a	54	0.7	21
d	46	0.6	18
d	54	0.2	11
e	57	0.6	20
f	59	— 0.6	neg.
g	45	0.5	16
i	49	0.3	13
i	63	0.2	12
l	44	0.5	17
Mean	52	0.34	14

c) From all values in tables a) and b)

Shock	h
a	14
d	15
e	17
g	15
i	10

VIII. The depths of foci.

There are many methods of finding out the focal depth of an earthquake, but in each particular case the number of practicable methods is very limited. As stated before, it is not possible in our case

to decide at what time the $\bar{S}$-waves arrive, or to find the difference in time between the arrival of these waves and the surface shear waves. Therefore, it is impossible to use any of these two kinds of waves, and in using microseismic data we can deal only with P. If we knew the

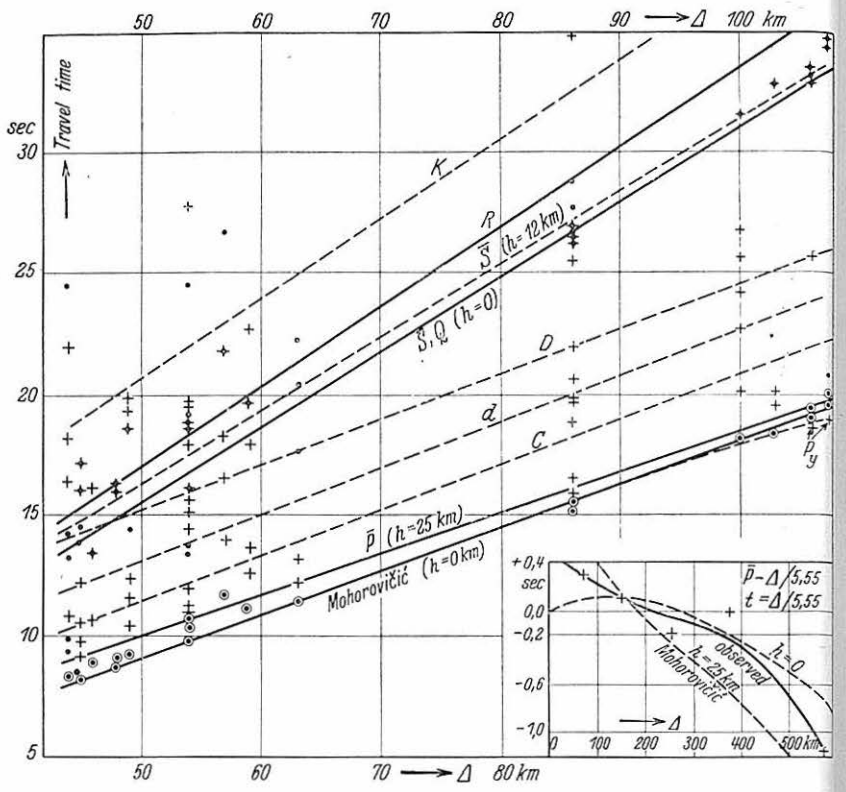

Fig. 7. Travel-times of waves in Southern California at distances less than 100 km. (Inset) Mean observed and calculated differences: Travel-time of $\bar{P}$ minus $\Delta/5.55$. (Δ = distance in km.)

thickness of the layers and the wave velocities we could also use the time differences between the different kinds of P-waves.

In figure 7 the travel times of the $\bar{P}$-waves are plotted against the distance. Here we also notice the travel time curves of these waves, found by MOHOROVIČIĆ for a focal depth of 0 and of 25 km. The observed values are generally between these two curves. In the small figure the travel times calculated by MOHOROVIČIĆ for the two values of focal depth h minus the value distance divided by 5.55 are plotted

against the distance, also the corresponding values (crosses) observed, according to the means of table VI. The full line gives the curve most likely to correspond to the observations. It runs between the curves calculated for focal depths of 0 and 25 km. From this figure we find therefore that evidently the wave velocity in the upper California layer is nearly the same as assumed by MOHOROVIČIĆ, and that the depth of focus is somewhat nearer to 0 than to 25 km., it having been near 10 km. If the curvature of the observed curve is true and not caused by errors of 0.2 seconds between 200 and 500 km., it would follow from observations that the increase of velocity with depth is somewhat less in the uppermost part of the first layer, than assumed by MOHOROVIČIĆ, and somewhat larger in the lower part of this layer.

In figure 7 all observations of all shocks are used. Now we must try to ascertain whether any differences existed between the different shocks. If we use only short distances, the depth of focus h is given within the limit of error of the observations by the formula

$$h^2 = (tv)^2 - \Delta^2$$

where t is the travel time of the $\overline{P}$-waves, v their mean velocity and Δ the distance. On the other hand we can express t by the travel time for the depth of focus zero and the difference d, which has been calculated in table VI for each seismogram:

$$t = \frac{\Delta}{v} + d\,.$$

Combining these two formulas we have

$$h^2 = vd\,(vd + 2\,\Delta)$$

or approximately in most cases $h^2 = 2\,vd\,\Delta$. With the first formula h has been calculated for all seismograms from distances less than 70 km. The values of d were taken from table VI. The results are given in table XVIIIb. They show that the depths of foci were the same in all cases, within the limits of error, the mean being 14 km.

Finally we can try to calculate the depths of foci from the macroseismic data. A formula for this purpose has been given by GASSMANN (6):

$$^1/_3\,(J - 2) = \log\left[\sqrt{1 + \left(\frac{r}{h}\right)^2} + 0.06\right]\sqrt{1 + \left(\frac{r}{h}\right)^2}$$

where J = maximum intensity of the shock, r = mean radius of the shaken area and 0.06 a factor of absorption according to GASSMANN's investigation of shocks in the Alps. The data and results in our case are found in table XVIIIa. Again the results agree within the limits

of error, the mean of 12 km. agrees very well with all results found previously by entirely different methods*).

Therefore it is very probable that all shocks originated at a depth between 10 and 15 km. We shall see that this is very near the lower surface of the first (granitic) layer, just as has been found for other countries.

IX. The thickness of layers in Southern California.

If the velocities of a certain kind of waves (either longitudinal or transversal) in successive layers are given by V_1, V_2, $V_3 \ldots$, V_n, we can calculate the thickness d_1, d_2, $d_3 \ldots$ of these layers, assuming constant velocity in each of them, in the following way:

First layer

$$2d_1 - h = \frac{\Delta^* \left(\frac{1}{V_1} - \frac{1}{V_2}\right)}{\sqrt{\frac{1}{V_1^2} - \frac{1}{V_2^2}}}.$$

where Δ^* = Distance where the travel time curves of the two corresponding waves intersect, h = depth of focus. For each following layer we have (i = angle of incidence)

$$\sin i_1 : \sin i_2 : \sin i_3 : \ldots : 1 = V_1 : V_2 : V_3 : \ldots : V_n$$

$$\Delta_n = (2\,d_1 - h)\,\mathrm{tg}\, i_1 + 2\,d_2\,\mathrm{tg}\, i_2 + 2\,d_3\,\mathrm{tg}\, i_3 + \ldots + 2\,d_{n-2}\,\mathrm{tg}\, i_{n-2}$$

$$t_n = \frac{2d_1 - h}{\cos i_1} + \frac{2d_2}{\cos i_2} + \frac{2d_3}{\cos i_3} + \cdots + \frac{2d_{n-2}}{\cos i_{n-2}}.$$

If t' is the travel time to a distance Δ' of the wave with its deepest point in the layer n, we calculate

$$D_n = \Delta' - \Delta_n \qquad T_n = t' - t_n$$

$$d_{n-1} = \frac{(V_n T_n - D_n)\cos i_{n-1}}{2\left(\frac{Vn}{Vn-1} - \frac{Vn-1}{Vn}\right)}.$$

Assuming that P_y, P_m, P_x and P_n, as well as the corresponding S-waves, are caused in this way, the following thicknesses of layers and corresponding wave velocities have been found:

*) For the South German Earthquake, November 16, 1911, we find by this method a focal depth of the order of 30 km., corresponding again with the results calculated by using the seismograms.

Thickness of layer	Velocity longitud.	Thickness of layer	Velocity transversal-	Mean lower depth	Veloc. long. by vel. transv.	Poissons ratio
0—14	5.55	0—13	3.23	14	1.70	0.24
14—26	6.05	13—24	3.39	25	1.79	0.27
26—30	6.83	24—32	3.66	31	1.86	0.30
30—39	7.6	32—38	4.24	39	1.80	0.27
>39	7.94	>38	4.45	—	1.78	0.27

For the first layer the calculations showed that $2d = h + 16$. As the focus must be situated within this layer, no P_m being observed otherwise, we find $h \leqq 16$ km. and $d_1 = \leqq 16$ km. So the thickness of this layer is rather certain. Assuming that the P_x- and S_x-waves are not caused by a layer, the third layer will extend from 25 to 36 km., and there the layer with a velocity of 7.94 km. for longitudinal waves will begin.

The thickness of 14 km. found for the first (granitic) layer agrees very well with the value of 15 km., found by BYERLY (3), WOOD and RICHTER (16) from blasts.

So far we have assumed that the velocity is constant in every layer. As a matter of fact, it increases with depth. The travel time curves of MOHOROVIČIĆ are based on the assumption of the velocity

$$v = 5.54 \left(\frac{r_0}{r}\right)^{4.05}$$

which means that the velocity of the longitudinal waves increases from 5.54 km./sec. at the surface to 5.59 km./sec. at a depth of 14 km.

If finally we now compare other values with those for California, it appears at first glance that there are more layers here than elsewhere. But it must be remembered that evidently some of the P^*-waves found in Europe correspond to our P_m-waves and others to our P_y-waves (fig. 4). It is quite probable that the upper (granitic) layer in California has a thickness of some 10 km. less than under the Alps. This granitic layer seems to be entirely absent in northern Germany, where the velocities found for the uppermost layer correspond to the velocities in the second layer in California. The following values have been found in other countries:

England (Jeffreys)			North Germany (Wiechert, Brockamp and Wölcken)		South Germany (Gutenberg)		
Depth km.	V. longit. km./sec.	$\mathfrak{V}$ transv. km./sec.	Depth	V. km./sec.	Depth km.	V. long. km./sec.	$\mathfrak{V}$ transv. km./sec.
0—10	5.4	3.3	0—8	6.0	0—30 ±	5.6	3.2
10—20	6.3	3.7	8—?	6.8	30—45 ±	$6^1/_4$	?
>20	7.8	4.35			>45	8.2	4.4

Schwadorf (Wien) (V. Conrad)		Tauern (V. Conrad)		Japan (Matuzawa, others)		
Depth km.	V. longit. km./sec.	Depth km.	V. longit. km./sec.	Depth km.	V. longit. km./sec.	$\mathfrak{V}$ transv. km./sec.
0—40 ±	5.6	0 —(40)	5.5	0—20 ±	5—$5^1/_2$	$3^1/_4$
40—50	6.47	(40)—(50)	$6^1/_4$	20—50 ±	6—$6^1/_4$	$3^3/_4$
>50	8.12	>(50)	7.83	>50 ±	$7^1/_2$—8	$4^1/_2$

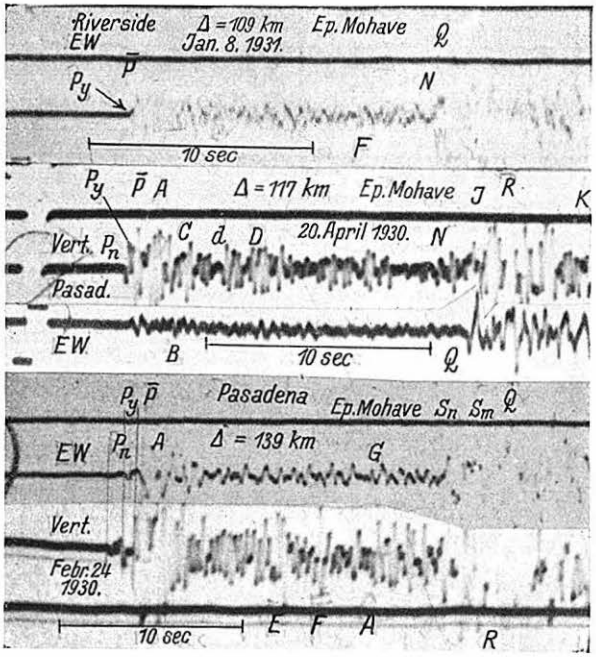

Fig. 8. Seismograms of earthquakes registered in Southern California; distance from the epicenter 109—139 km.

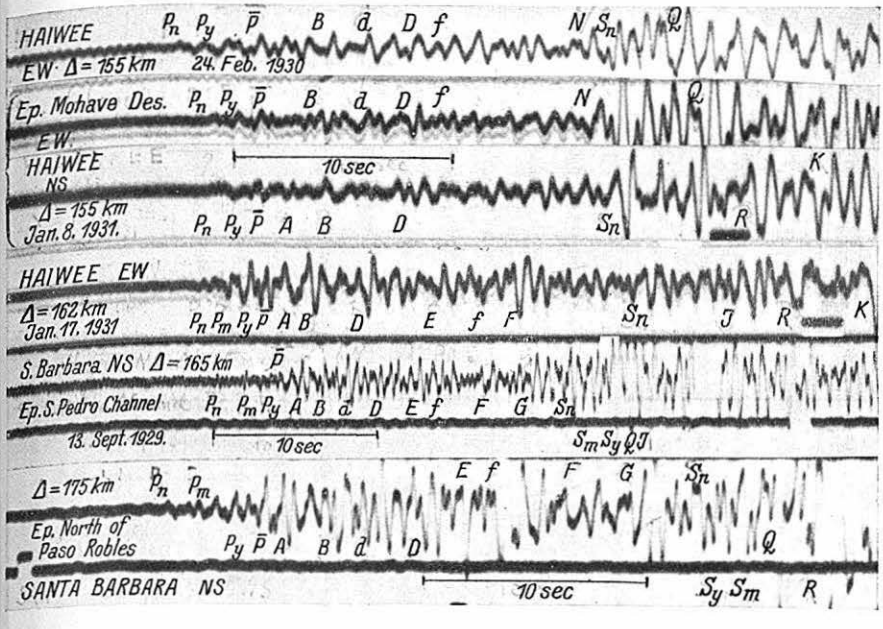

Fig. 9. Seismograms of earthquakes registered in Southern California; distance from the epicenter 155—175 km.

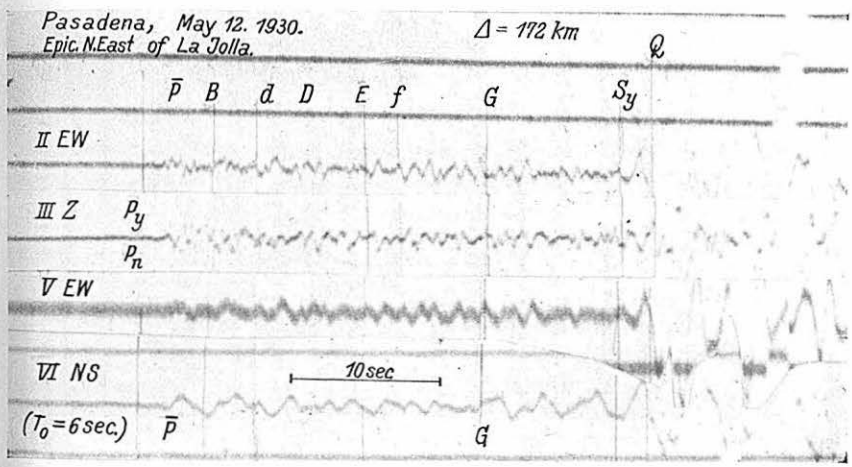

Fig 10. Seismograms of a shock, registered at Pasadena; distance 172 km. *II* = short period WOOD-ANDERSON torsion seismograph, *V* and *VI* = long period torsion instruments, *III* = vertical component, BENIOFF type.

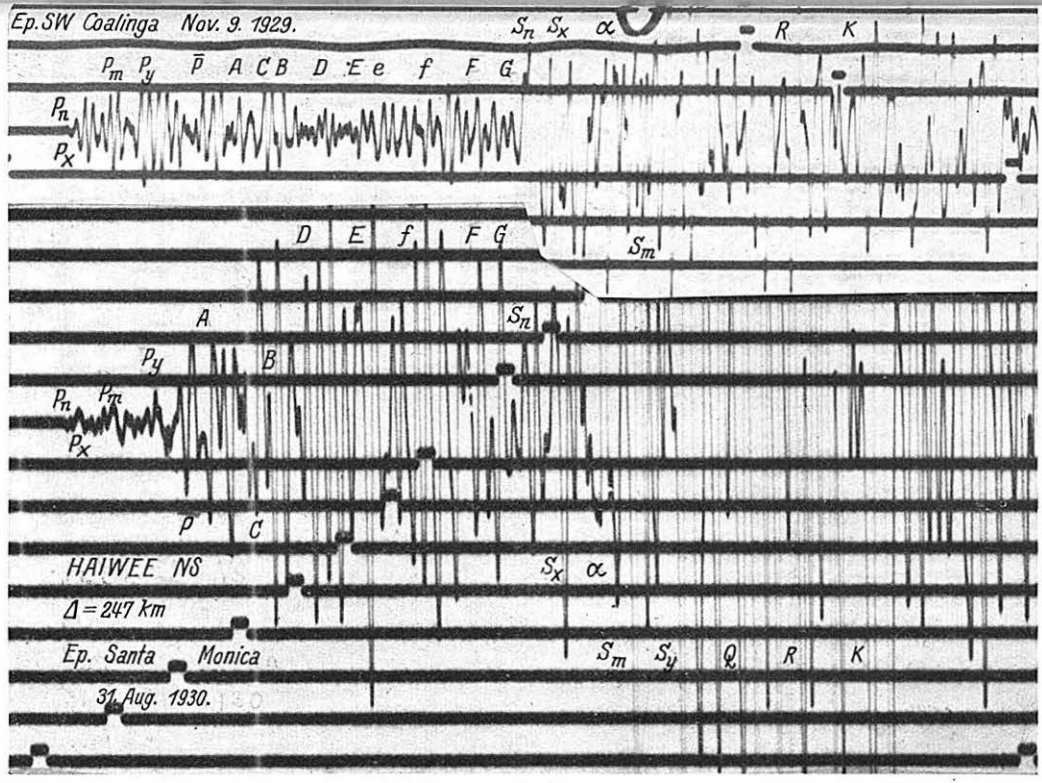

Fig. 11. Seismograms of shocks, distant 248 and 247 km., Southern California, registered by short period WOOD-ANDERSON torsion seismographs.

References.

1. H. P. Berlage, Bestimmung der Herdkoordinaten bei Nahbeben. Handbuch der Geophysik, hrsg. von B. Gutenberg, Verlag Gebr. Borntraeger, Berlin. Bd. 4, S. 500ff. 1930.
2. B. Brockamp und K. Wölcken, Bemerkungen zu den Beobachtungen bei Steinbruchsprengungen. Zeitschrift für Geophysik, 5, 163. 1929.
3. P. Byerly, Bulletin of the National Research Council, number 61, p. 88. Washington, July 1927.
4. V. Conrad, Gerl. Beitr., 20, 240. 1928.
5. — Laufzeitkurven des Tauernbebens . . . Mitt. der Erdbebenkomm. der Wiener Akad., N. F., Nr. 59. Wien 1925.
6. F. Gassmann, Jahresbericht 1925 des Erdbebendienstes der Schweiz. Meteorolog. Landesanstalt, Zürich. S. 14.
7. B. Gutenberg, Die Mitteleuropäischen Beben . . ., Veröff. des Zentralbüros der intern. Seismol. Assoc. Straßburg 1915.
8. — Gerl. Beitr., 23, 22. 1929.
9. — Handbuch der Geophysik, Bd. 4. Berlin 1930.
10. H. Jeffreys, Monthly Not. of Roy. Astron. Soc., Geophys. Supplem., London, 1, 483. 1927.
11. T. Matuzawa, Bull. of the Earthquake Res. Institute, Tokyo, 6, 177. 1929. — T. Matuzawa, K. Yamada, T. Suzuki, Bull. of the Earthquake Res. Inst. 7, 257. 1929.
12. A. Mohorovičić, Das Beben vom 8. X. 1909. Jahrbuch des met. Observat. Agram für das Jahr 1909. Zagreb 1910.
13. — Hodographes. Publ. Bureau Central Seismol. Int. Sér. A, fasc. 3. Paris 1925.
14. A. E. Mourant, Monthly Not. of the Roy. Astron. Soc., Geophys. Supplem., 2, 374. 1931.
15. R. Stoneley, Monthly Not. of the Roy. Astron. Soc., Geophys. Supplem., 2, 349. 1931.
16. H. O. Wood and Charles F. Richter, Bull. of the Seismol. Soc. of America, 21, 28. 1931.
17. N. W. Rajko, On the possibility of observing the phase of A. Mohorovičić ... Acad. des Sc. des Republ. Soviétiques Socialistes, Leningrad, Nr. 12, 1930.